Journal of Mining and Earth Sciences

Website: http://jmes.humg.edu.vn

Effect of soil Young's modulus on Sub-rectangular tunnels behavior under quasi-static loadings

Vi Van Pham [1], Anh Ngoc Do [1,*], Hung Trong Vo [1], Daniel Dias [2,3], Thanh Chi Nguyen [1], Do Xuan Hoi [1]

[1] *Faculty of Civil Engineering, Hanoi University of Mining and Geology, Vietnam*
[2] *School of Automotive and Transportation Engineering, Hefei Univ. of Technology, China*
[3] *Geotechnical expert, Antea Group, Antony, France*

ARTICLE INFO

Article history:
Received 18th Oct. 2021
Revised 28th Jan. 2022
Accepted 21st Mar. 2022

Keywords:
Numerical analysis,
Seismic load,
Sub-rectangular tunnel,
Tunnel lining.

ABSTRACT

Tunnels are an important component of the transportation and utility system of cities. They are being constructed at an increasing rate to facilitate the need for space expansion in densely populated urban areas and mega-cities. The circular and rectangular tunnels cannot completely meet the requirements of underground space exploitation regarding the cross-section. Sub-rectangular tunnels are recently used to overcome some drawbacks of circular and rectangular tunnels in terms of low utilization space ratio and stress concentration, respectively. However, the behavior of the sub-rectangular tunnels under seismic loading is still limited. This need to be regarded and improved. This paper focuses on conducting a numerical analysis to study the behavior of the sub-rectangular tunnels under seismic loadings. Here seismic loadings in this study are represented by quasi-static loadings. Based on the numerical model of the circular tunnel that was validated by comparison with analytical solutions, the numerical model of the sub-rectangular tunnel is created. This paper is devoted to highlight the differences between the behavior of the sub-rectangular tunnels compared with the circular ones subjected to quasi-static loadings. The soil-lining interaction, i.e., full slip and no-slip conditions are particularly considered. The influence of soil's Young's modulus on the sub-rectangular tunnel behavior under quasi-static loading is also investigated. The results indicated that soil's Young's modulus significantly affects static, incremental, and total internal forces in the tunnel lining under quasi-static loadings. Special attention is a significant difference in total internal forces in the sub-rectangular tunnel lining in comparison with the circular tunnel ones and the stability of the lining tunnel for both the full slip and no-slip conditions when subjected to quasi-static loadings.

*Corresponding author
E - mail: nado1977bb@gmail.com
DOI: 10.46326/JMES.2022.63(3a).02

1. Introduction

Urban underground structures are excavated at shallow depth and tunnel cross-sections are usually chosen as circular and rectangular shapes. The disadvantage of rectangular tunnels is stress concentration at four corners so the ability to work is worse than in circular tunnels (Nakamura et al., 2003). But compared with circular tunnels, the space utilization ratio of rectangular tunnels is much larger. Recently, special cross-section tunnels such as sub-rectangular tunnels have been applied and studied with real ratio or reduction ratio (Liu et al., 2018; Zhang et al., 2017; Zhu et al., 2017; Zhang et al., 2019), numerical analyses (Do et al., 2020; Nguyen et al., 2020). These cross-section tunnels have solved the drawback of the cross-section of circular and rectangular tunnels and also have advantages of those tunnels. It can work stably as a circular tunnel while also increasing the space utilization ratio as the rectangular tunnel.

The behavior of tunnel structures under seismic loading was thoroughly studied in the literature (Wang, 1993; Penzien, 2000; Bobet, 2003; FHWA, 2004; Hashash et al., 2001; Hashash et al., 2005; Naggar et al., 2008; Park et al., 2009; Sederat et al., 2009; Kouretzis et al., 2013; Nguyen et al., 2019; Sun et al., 2020; Tsinidis et al., 2020), there are research methods have high-level developed as experimental, analytical, numerical methods but these studies only researched for circular and rectangular tunnels. However, the behavior of the sub-rectangular tunnels under seismic loading is still limited. This need to be regarded and improved.

In this paper, a 2D finite-difference numerical model of circular and sub-rectangular tunnels under quasi-static loading is conducted. First of all, 2D finite-difference numerical is developed on a circular tunnel that internal forces on tunnel lining obtained compared to the results obtained using well-known analytical solutions (Wang, 1993; FHWA, 2004; Kouretzis et al., 2013). Based on the circular tunnel model, a sub-rectangular tunnel model is created. In addition, the effect of soil's Young's modulus on the behavior of tunnels under quasi-static loadings was carefully considered and evaluated. In this paper, the soil-lining interaction analytic is also attention. A significant difference in sub-rectangular tunnel behavior compared with the circular tunnel ones under quasi-static loadings based on numerical modeling.

2. Numerical models

2.1. Reference sub-rectangular tunnel case study- Shanghai metro tunnel

In this paper, the cross-section of the sub-rectangular tunnel was adopted from the literature of Do et al. (2020), which has been constructed in Shanghai, China. The dimensions of the sub-rectangular tunnel cross-section are 9.7 m in width and 7.2 m in height (Figure 1). In this study, a continuous lining was considered without taking the impact of joints into account. A cross-section of a circular tunnel with an external diameter of 9.76 m, which has an equivalent utilization space area, is taken into consideration based on the cross-section of the sub-rectangular tunnel (Figure 2).

2.2. Numerical model for the circular tunnel

First, a numerical simulation for a circular tunnel is carried out in this part using a finite difference program (FLAC^{3D}) (Itasca, 2012). The goal was to estimate internal forces in circular tunnel linings under quasi-static loading calculated by numerical solution compared with the ones calculated by an analytical solution, namely the solution of Wang (1993).

In Figure 3, a 2D plane strain model was developed by Do et al. (2015). The hexahedral zones are used for the volume under study. The embedded liner elements are used to describe the tunnel lining. These elements are attached to the zone faces along the tunnel boundary with interfaces. The soil-lining interface conditions were considered: no-slip and full slip conditions. The liner-zone interface stiffness (normal stiffness k_n and tangential stiffness k_s) is chosen using a rule of thumb (Itasca, 2012), k_n and k_s are set equal hundred times the equivalent stiffness of the stiffest neighboring zone (Itasca, 2012) for the no-slip condition case. When considering the full slip condition, k_s is assigned to be equal to zero.

The mesh is made up of a single layer of zones in the Y-direction, and when elements advance

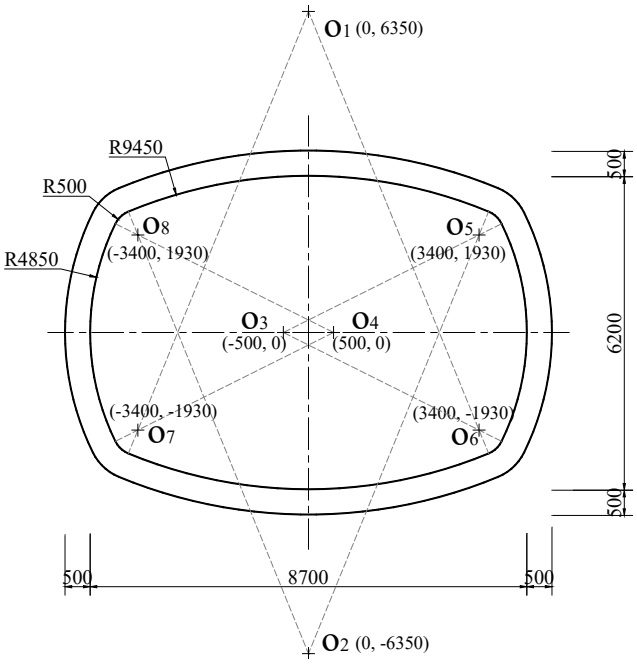

Figure 1. Sub-rectangular tunnel (Do et al., 2020).

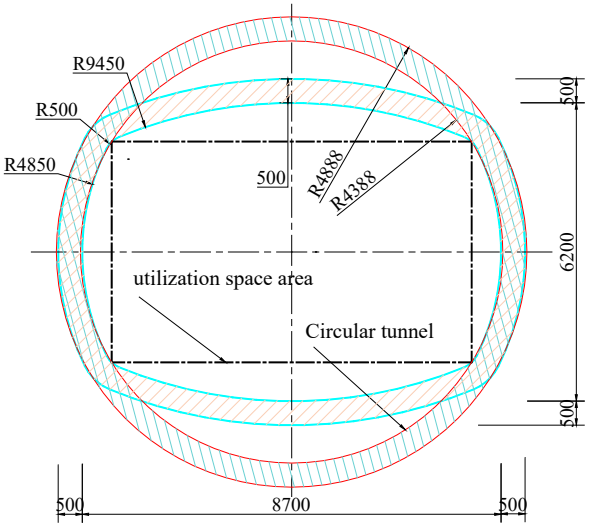

Figure 2. Circular tunnel with the same utilization space area.

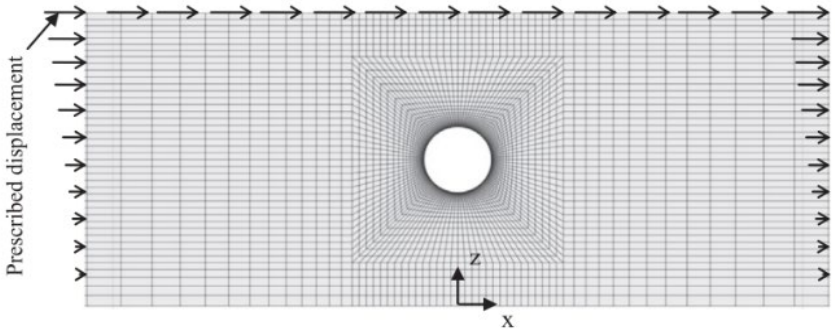

Figure 3. Geometry and quasi-static loading conditions for the circular tunnel model (Do et al., 2015).

away from the tunnel, their size of them increases (Figure 3). At boundary condition, the numerical model dimension is 120 m wide in the x-direction, and 40 m high in the z-direction, and the bottom of the model is blocked in all directions. It consists of 4800 zones and 9802 nodes.

In this paper, like in previous research with circular tunnels, ovaling deformations due to the quasi-static loading are imposed as inverted triangular displacements, along with the model lateral boundaries. Along the top boundary, uniform horizontal displacements are applied (Sederat et al., 2009; Do et al., 2015; Naggar and Hinchberger, 2012) (Figure 3). The magnitude of the prescribed displacements assigned at the top of the model is dependent on the maximum shear strain, γ_{max}, estimated based on the horizontal acceleration a_H and properties of the soil mass. Details of the mathematical formulation of the maximum shear strain, γ_{max}, are not presented in this paper. Readers can refer to the work by Wang, (1993), Hashash et al. (2001, 2005).

The first step of the numerical simulation process is to set up the model and assign the plane strain boundary conditions and the initial stress state taking into consideration the gravity field. Next step, the tunnel is excavated and the lining is assigned. Finally, the prescribed displacements are assigned on the model boundaries by the quasi-static loading that induced ovaling deformations.

2.3. Comparison between the numerical and analytical solutions for the circular tunnel case

The analytical solution presented by Wang (1993) and then later synthesized in FHWA (2004) was used for validation purposes of the numerical model exposed to quasi-static loading. The study's input data displayed in Table 1 were used as the reference case. In numerical models, it is presumable that the properties of the soil and tunnel lining materials are linear elastic. The analytical solution likewise used these presumptions. An anisotropic stress field was assigned in the numerical model with a lateral earth pressure coefficient, K_0 equal to 0.5. The horizontal acceleration, a_H equal to 0.5g, corresponds to the maximum shear strain γ_{max} of 0.38%.

The distribution of the incremental internal forces induced in the circular tunnel lining under quasi-static loading is illustrated in Figure 4. Both no-slip and full slip conditions between lining and soil interaction were considered when using the analytical solution and Flac^{3D}. The parameters of soil and tunnel lining in Table 1 are adopted. It can be seen that the results obtained by numerical and analytical solutions are in very good agreement, the discrepancies are under 2%. Both maximum and minimum extreme internal forces are interesting. They are named 'extreme incremental internal forces'. Similarly, 'extreme total internal

Table 1. Input parameters for the reference case study.

TT	Parameter	Symbol	Unit	Value
	Soil properties			
1	Unit weight	γ	MN/m^3	0.018
2	Young's modulus	E	MPa	100
3	Poisson's ratio	ν	-	0.34
4	Internal friction angle	ϕ	degrees	33
5	Cohesion	c	MPa	0
6	Lateral earth pressure coefficient	K_0	-	0.5
7	Depth of tunnel	H	m	20
8	Peak horizontal acceleration at ground surface	a_H	g	0.5
9	Moment magnitude	M_w		7.5
10	Source to site distance		km	10
	Tunnel lining properties			
11	Young's modulus	E_l	MPa	35000
12	Poisson's ratio	ν_l	-	0.15
13	Lining thickness	t	m	0.5
14	External diameter	D	m	9.76

forces' represent both the maximum and minimum total internal forces induced in the tunnel lining.

Figure 4a illustrates that the absolute extreme incremental bending moments in the full slip condition are larger than the ones obtained in the no-slip condition, 14%. However, compared to the no-slip condition, the absolute extreme incremental normal forces in the full slip condition are substantially lower (Figure 4b).

3. Constructing a numerical model for sub-rectangular tunnels

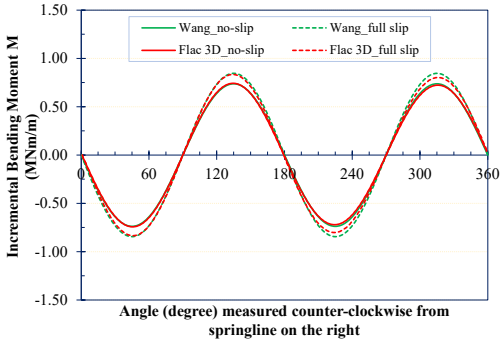

(a) Incremental bending moments.

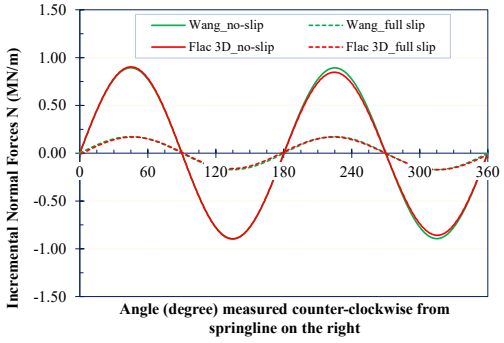

(b) Incremental Normal Forces.

Figure 4. Distribution of the incremental internal forces in the circular tunnel obtained by Flac3D and Wang solution.

In this section, Similar to the circular tunnel model under quasi-static loading, a numerical model for the sub-rectangular tunnel was created. It only changes the geometry of the circular tunnel into a sub-rectangular shape (Figure 5). The geometry parameters of sub-rectangular tunnels are illustrated in Figure 1 and other parameters are presented in Table 1. The numerical model is consisting of 5816 elements and 11870 nodes. The bottom of the model was blocked in all directions, while the vertical sides were fixed to their horizontal side. The magnitude of the prescribed displacements assigned to the sub-rectangular tunnel model is also similar to the circular tunnel model under quasi-static loading.

3.1. Comparison between circular and sub-rectangular tunnels under quasi-static loading

Figure 6 illustrates the static bending moments and normal forces in the circular and sub-rectangular tunnel linings under static loading. While Figures 7 and 8 describe the incremental and total bending moments and normal forces in these tunnel linings under quasi-static loading. Both no-slip and full slip conditions have also been considered. Input data of the reference case was presented in Table 1.

Figure 6 indicated that the static bending moments in the circular tunnel lining are smaller than the ones in the sub-rectangular tunnel lining for both no-slip and full slip conditions, the maximum static bending moments are observed at 90 and 270 degrees corresponding with the crown, and bottom of the circular and sub-rectangular tunnels. By contrast, the static normal forces in the sub-rectangular tunnel lining are smaller than the ones in the circular tunnel for both no-slip and full slip conditions.

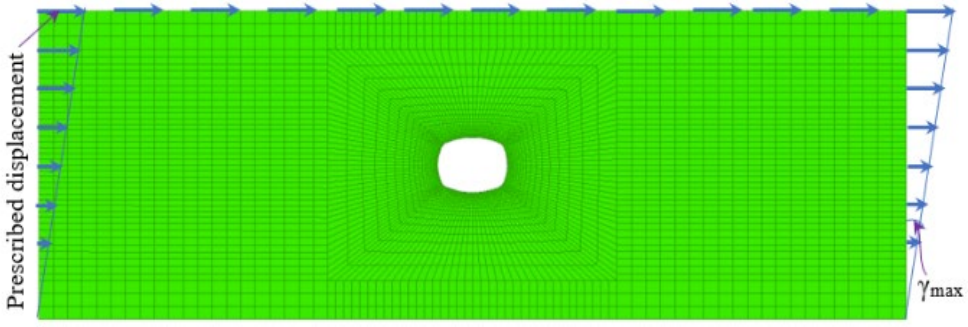

Figure 5. Geometry and quasi-static loading conditions in the numerical model of a sub-rectangular tunnel.

Considering the influence of the soil-lining interaction, the static bending moments in the tunnel lining in the full slip condition are slightly larger than the ones in the no-slip condition, these differences are 13% and 7% corresponding to the circular and sub-rectangular tunnels, respectively (Figure 6a).

Figure 6b indicated that the soil-lining interaction significantly influenced the static normal forces in the tunnel linings. The maximum normal forces obtained in the no-slip condition are much larger than the ones in the full slip condition, while the minimum static normal forces in the full slip condition are significantly larger compared to the ones in the no-slip condition, corresponding to 45% and 51% for the circular and sub-rectangular tunnels respectively. The most changes are observed at the crown and bottom areas of the tunnel cross-sections. It could be identified that the circular tunnels are more stable than the sub-rectangular tunnels under static loadings, and the tunnel works more stable in the no-slip condition compared to the one in the full slip condition.

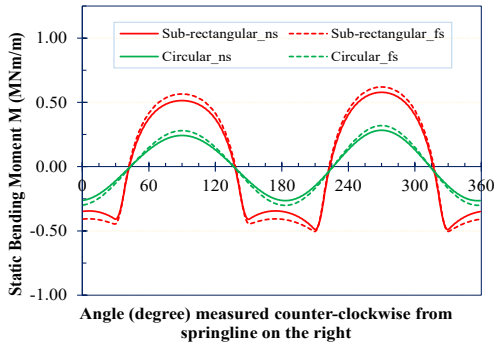

(a) Static bending moments.

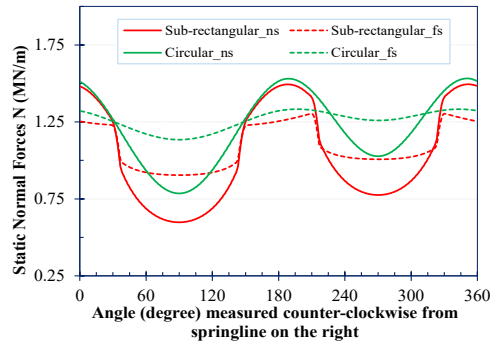

(b) Static normal forces.

Figure 6. Distribution of the static bending moments and normal forces in the sub-rectangular and circular tunnels.

Figure 7 shows at the corners of the sub-rectangular tunnel cross-section appeared the extreme incremental bending moments and normal forces. The difference with the sub-rectangular tunnel, the positions of the extreme incremental and normal forces are observed on the circular tunnel lining making an angle of 45 degrees with the horizontal. There is a special note in Figure 7a, that the absolute extreme bending moments on the sub-rectangular tunnel lining in the no-slip condition are larger than the ones in the full slip condition. This is the opposite with the case of the extreme incremental bending moments on the circular tunnel lining (Figure 7a).

In the no-slip condition, the absolute extreme bending moments in the sub-rectangular tunnel lining are larger by 20% than the ones in the circular tunnel lining. By contrast, compared to the circular tunnel in the full slip condition, the absolute extreme bending moment on the sub-rectangular tunnel lining are smaller by 4%. According to Figure 7b, the incremental normal forces in tunnel linings in the full slip condition are significantly smaller than in the cases of the no-slip condition.

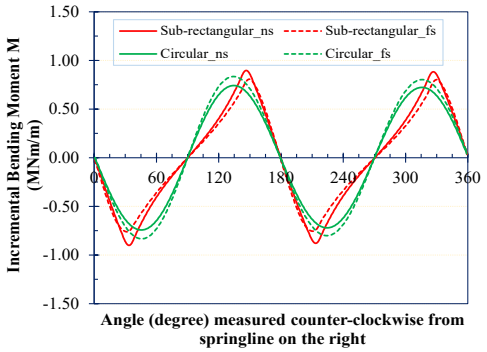

(a) Incremental bending moments.

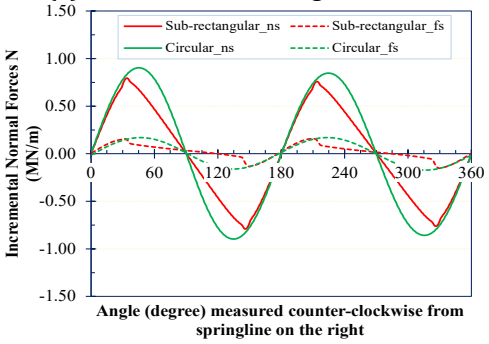

(b) Incremental normal forces.

Figure 7. Distribution of the incremental bending moments and normal forces in the sub-rectangular and circular tunnels.

There is almost no difference between the absolute extreme normal forces on both two tunnel linings in the full slip condition. The absolute extreme normal forces in the circular tunnel lining in the no-slip condition are 9% more than the ones in the sub-rectangular tunnel lining (Figure 7b).

Figure 8 shows an overview of the difference between total internal forces in the circular and sub-rectangular tunnel linings under quasi-static loading. The total internal forces are equal to the static internal forces plus the incremental internal forces in the tunnel linings. Figure 8a indicated that the minimum total bending moments in the sub-rectangular tunnel lining appear at the shoulders of the tunnel cross-section. Compared to the minimum total bending moments in the circular tunnel lining, the ones in the sub-rectangular tunnel are smaller at 71% and 42% corresponding to no-slip and full slip conditions. By contrast, the maximum total bending moments are almost constant in two tunnel linings in the no-slip condition, while for the full slip condition,

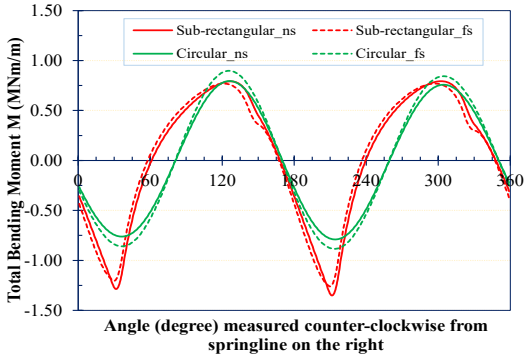

(a) Total bending moments.

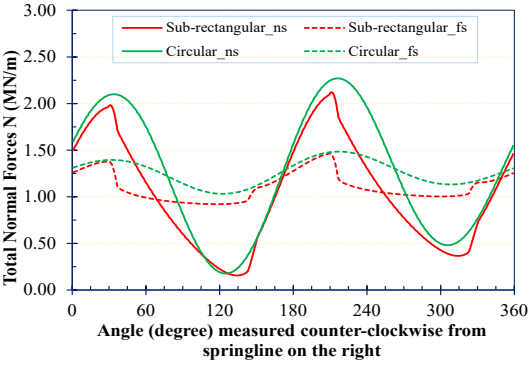

(b) Total normal forces.

Figure 8. Distribution of the total bending moments and normal forces in the sub-rectangular and circular tunnels.

the maximum total bending moments in the circular tunnel lining are larger by 14% than the one in the sub-rectangular lining.

Figure 8b illustrated the difference in the total normal forces in the circular and sub-rectangular tunnel linings. The maximum and minimum total normal forces in tunnel lining in the full slip condition are significantly lower than the ones in the no-slip condition. Compared to the circular tunnel lining, the maximum total normal forces in the sub-rectangular lining are smaller at 6.5% and 1.4% corresponding to the no-slip and full slip conditions. Similarly, the minimum total normal forces on the circular tunnel lining are larger than the ones on the sub-rectangular tunnel lining for both no-slip and full slip conditions corresponding to 11.5% and 10.7%.

In the next section below, the effect of soil's Young's modulus on the circular and sub-rectangular tunnel behavior was conducted. While the effect of the soil-lining interaction condition was also considered.

3.2. Effect of the soil's Young's modulus (E)

The soil's Young's modulus values are assumed to range between 10 and 350 MPa, corresponding to the shear strains, γ_{max}, of 1.21÷0.21% while keeping the a_H value equal to 0.5g. The other parameters of the reference case presented in Table 1 are adopted. The total internal forces on the circular and sub-rectangular tunnel linings are shown in Figures 9 to 14.

Figures 9, 10, 11, and 12 have presented the total internal forces induced in the circular and sub-rectangular tunnel linings under quasi-static loading for both the no-slip and full slip conditions when the *E* values vary from 10÷350 MPa. Figures 9a to 12a indicated that the *E* values increase causes a decrease in the absolute extreme total bending moment in both tunnel linings. This trend is also suitable for the total normal forces in the circular and sub-rectangular tunnel linings in full slip condition (Figures 10b, 12b). By contrast, the maximum total normal forces in the circular and sub-rectangular tunnel linings have the same trend to increase with an increase in the *E* values of soil (Figures 9b,11b).

Figures 9 and 10 also show that the positions of the extreme total bending moments and normal

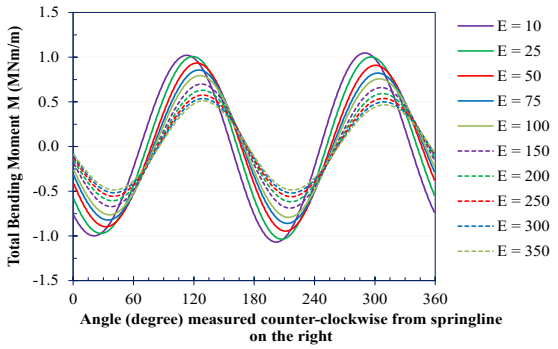

(a) Total bending moments.

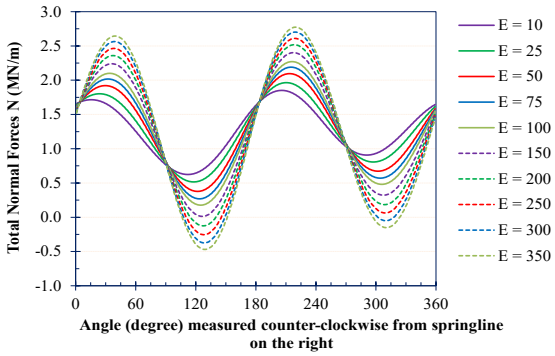

(b) Total normal forces.

Figure 9. Effect of the E values on the total internal forces for the circular tunnel lining in the no-slip condition.

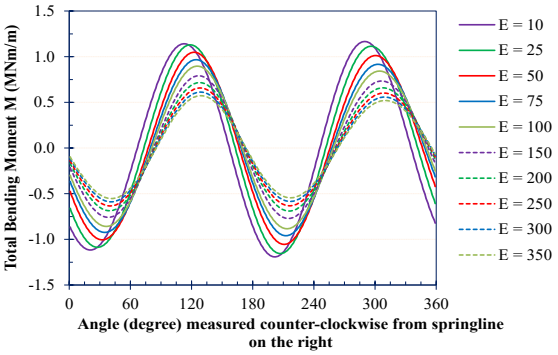

(a) Total bending moments.

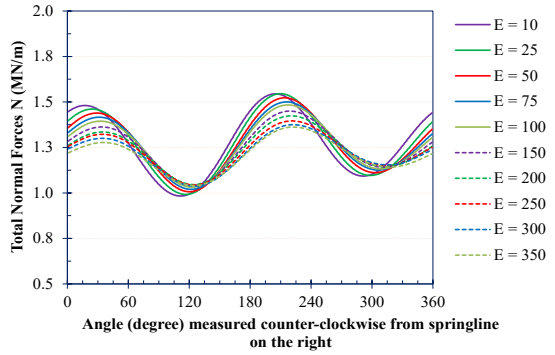

(b) Total normal forces.

Figure 10. Effect of the E values on the total internal forces for the circular tunnel lining in the full slip condition.

forces observed on the circular lining vary when the *E* values change. These positions make an angle with the horizontal vary from 25÷40 degrees corresponding to the *E* values from 10÷350 MPa. These tend are suitable in both the no-slip and full slip conditions.

It can be explained that the extreme total internal forces in the tunnel linings depend on the values of the static and incremental internal forces when the tunnel linings are subjected to static and quasi-static loadings. It means that the position of the extreme total internal forces tends to shift towards the positions of the extreme incremental internal forces when the extreme incremental internal forces increases compared to the extreme static internal forces.

Compared to the total internal forces in the circular tunnel lining, there is a clear difference in the position of the extreme total bending moments and normal forces in the sub-rectangular tunnel lining. The positions of the minimum total bending moments in the sub-rectangular tunnel are always at the shoulder of the tunnel cross-section. While these positions of the maximum total bending moments vary from 77÷37 degrees making an angle with the horizontal corresponding to the *E* values increase from 10÷350 MPa (Figures 11a and 12a). However, the shoulders of the sub-rectangular tunnel cross-section are the positions of the extreme total normal forces in no-slip condition and the maximum total normal forces in full slip condition (Figures 11b and 12b).

Figures 13, 14 illustrated the extreme total internal forces in the circular tunnel lining compared with the sub-rectangular tunnel lining under quasi-static loadings in the no-slip and full slip conditions. The minimum total bending moments in the circular tunnel lining are larger than the ones in the sub-rectangular tunnel lining for both the no-slip and full slip conditions. These differences vary from 51÷101% in the no-slip

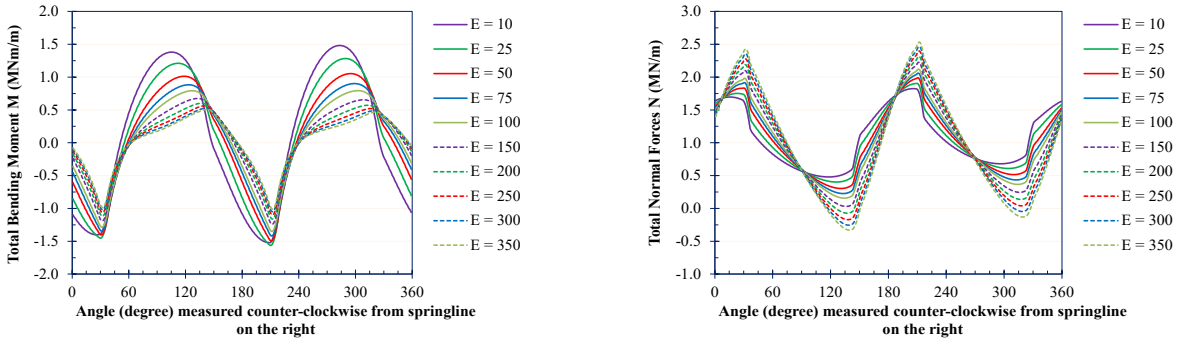

a) Total bending moments, *b) Total normal forces.*

Figure 11. Effect of the E value on the total internal forces for the sub-rectangular tunnel lining in the no-slip condition.

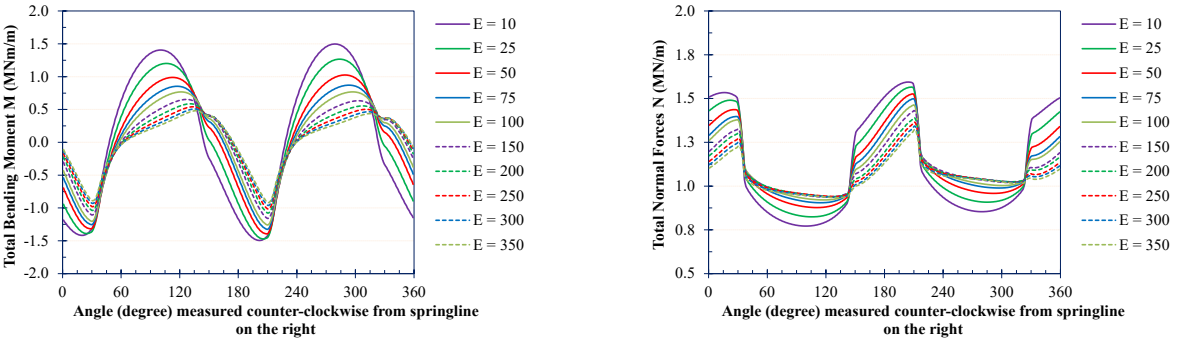

a) Total bending moments. *b) Total normal forces.*

Figure 12. Effect of the E value on the total internal forces for the sub-rectangular tunnel lining in the full slip condition.

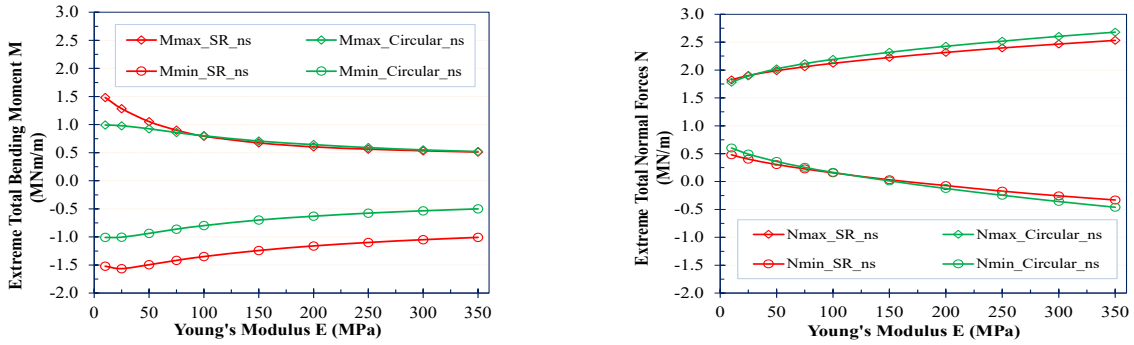

(a) Total bending moments. *(b) Total normal forces.*

Figure 13. Effect of the E values on the extreme total internal forces for the circular and sub-rectangular tunnel linings in the no-slip condition.

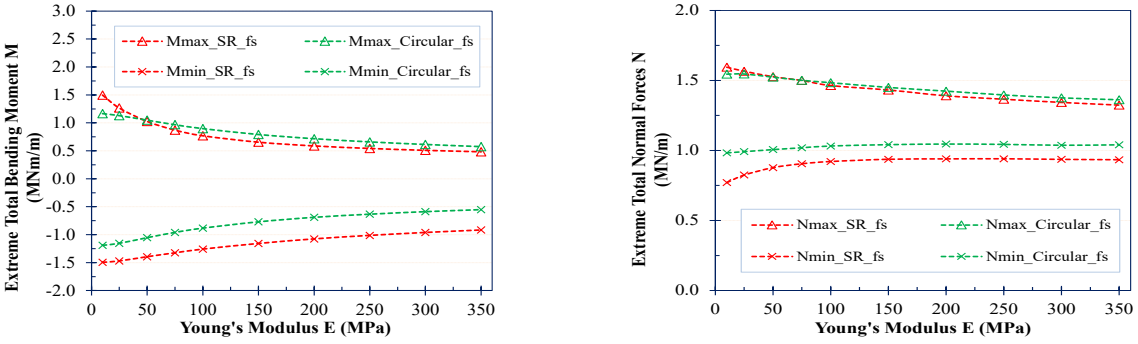

(a) Total bending moments. *(b) Total normal forces.*

Figure 14. Effect of the E values on the extreme total internal forces for the circular and sub-rectangular tunnel linings in the full slip condition.

condition compared to 26÷66% in the full slip condition when the *E* values change from 10÷350 MPa (Figures 13a, 14a).

For the no-slip condition, when the *E* values are more than 100 MPa, the maximum total bending moments in circular tunnel lining are larger than the ones in the sub-rectangular tunnel lining under 6%. Similarly, for the full slip condition, the maximum total bending moments in circular tunnel lining are larger than the ones in the sub-rectangular tunnel lining from 2÷16% corresponding to the *E* values from 50÷350 MPa (Figures 13a, 14a).

The extreme total normal forces in the tunnel linings are not much different between the circular and sub-rectangular tunnels in the no-slip condition. This is similar to the maximum total normal forces in the full slip condition (Figures 13b, 14b). For the full slip condition, the minimum total normal forces in the circular tunnel lining are larger than the ones in the sub-rectangular tunnel lining from 22÷10% corresponding to the E values vary from 10÷350 MPa.

4. Conclusion

The behavior of the circular and sub-rectangular tunnel linings is investigated by a 2D numerical study under quasi-static loading. The influences of soil's Young's modulus and the soil-lining interaction conditions on the behavior of the tunnel linings under quasi-static loadings have also been investigated. The response of the circular tunnel compared to the sub-rectangular tunnel was considered. There are some conclusions following:

- The Soil's Young's modulus, *E*, has a significant effect on the total internal forces in both the circular and sub-rectangular tunnel linings for both no-slip and full slip conditions under quasi-static loading;

- There is a complete difference between the sub-rectangular and circular tunnel behaviors under quasi-static loading in both the no-slip and full slip conditions. The absolute extreme total bending moments in the circular tunnel lining for the full slip condition are larger than the ones in the no-slip condition, while the absolute extreme total bending moments in the sub-rectangular tunnel lining in the full slip condition are smaller than the ones in the no-slip condition;

- The positions of the extreme total bending moments and normal forces observed on the tunnel linings vary when the *E* values change. It can be explained that the extreme total internal forces in the tunnel linings depend on the values of the static and incremental internal forces in the tunnel linings under static and quasi-static loadings;

- The absolute extreme total normal forces in the tunnel linings in the no-slip condition are always larger than the ones in the full slip. It is suitable for both circular and sub-rectangular tunnels cases;

- The absolute extreme total bending moments in the circular and sub-rectangular tunnel linings tend to decrease gradually corresponding to an increase of the *E* values under quasi-static loadings.

- The soil's Young's modulus, *E*, increases induced to the absolute extreme total normal forces in the tunnel linings increase for both the sub-rectangular and circular tunnels (no-slip condition). For the full slip condition, there is a slight decrease in the maximum total normal forces in the tunnel linings, and an insignificant change in the minimum total normal forces in the ones is observed.

The numerical results obtained in this study are useful for the preliminary design of the circular and sub-rectangular tunnel linings under quasi-static loadings.

Acknowledgments

This first author was funded by Vingroup JSC and supported by the Master, PhD Scholarship Programme of Vingroup Innovation Foundation (VINIF), Institute of Big Data, code VINIF.2021.TS.167.

Author Contributions

Vi Van Pham - data curation, formal analysis, investigation, software, validation, writing original draft; Anh Ngoc Do - methodology, conceptualization, formal analysis, supervision, writing, review & editing; Hung Trong Vo - conceptualization, supervision, writing – review & editing; Daniel Dias - supervision, writing, review & editing; Thanh Chi Nguyen - visualization,

validation, writing, review & editing; Hoi Xuan Do - validation.

References

Bobet, A. (2003). Effect of pore water pressure on tunnel support during static and seismic. *Tunnelling and Underground Space Technology 18*, 377-393.

Do, N. A., Dias, D., Zixin, Z., Xin, H., Nguyen T. T., Pham V. V., & Ouahcène, N. R. (2020). Study on the behavior of squared and sub-rectangular tunnels using the Hyperstatic Reaction Method. *Transportation Geotechnics,* 22.

Do N. A., Dias D., Oreste P. P., & Djeran-Maigre I. (2015). 2D Numerical Investigation of Segmental Tunnel Lining under Seismic Loading. *Soil Dynamics and Earthquake Engineering,* 72, 66-76.

FHWA. (2004). Seimic retrofitting manual for highway struttures: Part 2 – retaining strutures, slopes, tunnels, culverts, and roadways. *U.S. Department of transportation. Federal Highway Administration*. Publication No. FHWA-HRT-05-067.

Hashash, Y. M. A., Hook, J. J., Schmidt, B., & Yao, J. I. C. (2001). Seismic design and analysis of underground structures. *Tunnelling and Undergound Space Technology, 16*, 247–293.

Hashash, Y. M. A., Park, D., & Yao, J. I. C. (2005). Ovaling deformations of circular tunnels under seismic loading, an update on seismic design and analysis of underground structures. *Tunnelling and Underground Space Technology, 20*, 435-441.

Itasca Consulting Group. (2012). *FLAC Fast Lagrangian Analysis of Continua, Version 5.0*. User's manual, Available: ⟨http.itascacg.com⟩.

Kouretzis, G., Sloan, S. W., & Carter, J. P. (2013). Effect of interface friction on tunnel liner internal forces due to seismic S- and P-wave propagation. *Soil Dynamic and Earthquake Engineering, 46*, 41-51.

Liu, X., Ye, Y., Liu, Z., & Huang, D. (2018). Mechanical behavior of Quasi-rectangular segmental tunnel linings: First results from full-scale ring tests. *Tunn. Undergr. Space Technol, 71*, 440-454.

Naggar, H. E., & Hinchberger, S. D. (2012). Approximate evaluation of stresses in degraded tunnel linings. *Soil Dynamics and Earthquake Engineering, 43*, 45-57.

Naggar, H. E., Hinchberge, S. D., Hesham, M., & Naggar, E. I. (2008). Simplified analysis of sesmic in-plane stresses in composite and jointed tunnel linings. *Tunnelling and Underground Space Technology, 28*, 1063-1077.

Nakamura, H., Kubota, T., & Furukawa, M. (2003). Unified construction of running track tunnel and crossover tunnel for subway by rectangular shape double track cross-section shield machine. *Tunnelling and Underground Space Technology, 18*(2), 253-262.

Nguyen, D. D., Park, D., Shamsher, S., Nguyen, V. Q., & Lee, T. H. (2019). Seismic vulnerability assessment of rectangular cut-and-cover subway tunnels. *Tunnelling and Underground Space Technology, 86*, 247–261.

Nguyen, T. T., Do, N. A., Karasev, M. A., Dang, V. K., & Dias, D. (2020). Tunnel Shape Influence on the Tunnel Lining Behavior. *Proceeding of ICE - Geotechnical Engineering*. doi.org/10.1680/jgeen.20.00057.

Park, K. H., Tantayopin, K., Tontavanich, B., & Owatsiriwong, A. (2009). Analytical solution for seismic-induced ovaling of circular tunnel lining under no-slip interface conditions: A revisit. *Tunnelling and Underground Space Technology, 24*, 231-235.

Penzien, Z. (2000). Seismically induced racking of tunnel linings. *Int. J. Earthquake Eng. Struct. Dynamic, 29*, 683-691.

Sederat, H., Kozak, A., Hashash, Y. M. A., Shamsabadi, A., & Krimotat, A. (2009). Contact interface in seismic analysis of circular tunnels. *Tunnelling and Underground Space Technology, 24*, 482-490.

Sun, Q. Q., Du, D., & Dias, D. (2020). An improved Hyperstatic Reaction Method for tunnels under seismic loading. *Tunnelling and*

Underground Space Technology. DOI: 10.1016/j.tust.2020.103687.

Tsinidis, G., Silva, F. D., Anastasopoulos, I., & Bilotta, E. (2020). Seismic behavior of tunnels: From experiments to analysis. *Tunnelling and Underground Space Technology, 99*, 103334.

Wang, J. N. (1993). Seismic design of tunnels: A state-of-the-art approach, *Brinckerhoff Quade and Douglas Inc., New York*.

Zhang, Z. X., Zhu, Y. T., & Zhu, Y. F. (2017). Development and application of a 1:1 mechanical test system for special-shaped shield lining with a large cross-section. *Chinese Journal of Rock Mechanics and Engineering, 12*(36), 2895-2905. (in Chinese)

Zhu, Y. T., Zhang, Z. X., & Zhu, Y. F. (2017). Capturing the cracking characteristics of concrete lining during prototype tests of a special-shaped tunnel using 3D DIC photogrammetry, *Eur J Environ Civ Eng,* 1–21.

Zhang, Z., Zhu, Y., Huang, X., Zhu, Y., & Liu, W. (2019). "Standing" full-scale loading tests on the mechanical behavior of a special-shape shield lining under shallowly-buried conditions. *Tunnelling and Underground Space Technology, 86*(1), 34-50.